

# Measurements of the absolute branching fractions for $D \rightarrow \bar{K}\pi e^+\nu_e$ , $D \rightarrow \bar{K}^* e^+\nu_e$ and determination of $\Gamma(D^+ \rightarrow \bar{K}^{*0} e^+\nu_e)/\Gamma(D^+ \rightarrow \bar{K}^0 e^+\nu_e)$

(BES Collaboration)

M. Ablikim<sup>1</sup>, J. Z. Bai<sup>1</sup>, Y. Ban<sup>12</sup>, J. G. Bian<sup>1</sup>, X. Cai<sup>1</sup>, H. F. Chen<sup>16</sup>, H. S. Chen<sup>1</sup>, H. X. Chen<sup>1</sup>, J. C. Chen<sup>1</sup>, Jin Chen<sup>1</sup>, Y. B. Chen<sup>1</sup>, S. P. Chi<sup>2</sup>, Y. P. Chu<sup>1</sup>, X. Z. Cui<sup>1</sup>, Y. S. Dai<sup>18</sup>, L. Y. Diao<sup>9</sup>, Z. Y. Deng<sup>1</sup>, Q. F. Dong<sup>15</sup>, S. X. Du<sup>1</sup>, J. Fang<sup>1</sup>, S. S. Fang<sup>2</sup>, C. D. Fu<sup>1</sup>, C. S. Gao<sup>1</sup>, Y. N. Gao<sup>15</sup>, S. D. Gu<sup>1</sup>, Y. T. Gu<sup>4</sup>, Y. N. Guo<sup>1</sup>, Y. Q. Guo<sup>1</sup>, K. L. He<sup>1</sup>, M. He<sup>13</sup>, Y. K. Heng<sup>1</sup>, H. M. Hu<sup>1</sup>, T. Hu<sup>1</sup>, G. S. Huang<sup>1a</sup>, X. T. Huang<sup>13</sup>, X. B. Ji<sup>1</sup>, X. S. Jiang<sup>1</sup>, X. Y. Jiang<sup>5</sup>, J. B. Jiao<sup>13</sup>, D. P. Jin<sup>1</sup>, S. Jin<sup>1</sup>, Yi Jin<sup>8</sup>, Y. F. Lai<sup>1</sup>, G. Li<sup>2</sup>, H. B. Li<sup>1</sup>, H. H. Li<sup>1</sup>, J. Li<sup>1</sup>, R. Y. Li<sup>1</sup>, S. M. Li<sup>1</sup>, W. D. Li<sup>1</sup>, W. G. Li<sup>1</sup>, X. L. Li<sup>1</sup>, X. N. Li<sup>1</sup>, X. Q. Li<sup>11</sup>, Y. L. Li<sup>4</sup>, Y. F. Liang<sup>14</sup>, H. B. Liao<sup>1</sup>, B. J. Liu<sup>1</sup>, C. X. Liu<sup>1</sup>, F. Liu<sup>6</sup>, Fang Liu<sup>1</sup>, H. H. Liu<sup>1</sup>, H. M. Liu<sup>1</sup>, J. Liu<sup>12</sup>, J. B. Liu<sup>1</sup>, J. P. Liu<sup>17</sup>, Q. Liu<sup>1</sup>, R. G. Liu<sup>1</sup>, Z. A. Liu<sup>1</sup>, Y. C. Lou<sup>5</sup>, F. Lu<sup>1</sup>, G. R. Lu<sup>5</sup>, J. G. Lu<sup>1</sup>, C. L. Luo<sup>10</sup>, F. C. Ma<sup>9</sup>, H. L. Ma<sup>1</sup>, L. L. Ma<sup>1</sup>, Q. M. Ma<sup>1</sup>, X. B. Ma<sup>5</sup>, Z. P. Mao<sup>1</sup>, X. H. Mo<sup>1</sup>, J. Nie<sup>1</sup>, H. P. Peng<sup>16d</sup>, R. G. Ping<sup>1</sup>, N. D. Qi<sup>1</sup>, H. Qin<sup>1</sup>, J. F. Qiu<sup>1</sup>, Z. Y. Ren<sup>1</sup>, G. Rong<sup>1</sup>, L. Y. Shan<sup>1</sup>, L. Shang<sup>1</sup>, C. P. Shen<sup>1</sup>, D. L. Shen<sup>1</sup>, X. Y. Shen<sup>1</sup>, H. Y. Sheng<sup>1</sup>, H. S. Sun<sup>1</sup>, J. F. Sun<sup>1</sup>, S. S. Sun<sup>1</sup>, Y. Z. Sun<sup>1</sup>, Z. J. Sun<sup>1</sup>, Z. Q. Tan<sup>4</sup>, X. Tang<sup>1</sup>, G. L. Tong<sup>1</sup>, D. Y. Wang<sup>1</sup>, L. Wang<sup>1</sup>, L. L. Wang<sup>1</sup>, L. S. Wang<sup>1</sup>, M. Wang<sup>1</sup>, P. Wang<sup>1</sup>, P. L. Wang<sup>1</sup>, W. F. Wang<sup>1b</sup>, Y. F. Wang<sup>1</sup>, Z. Wang<sup>1</sup>, Z. Y. Wang<sup>1</sup>, Zhe Wang<sup>1</sup>, Zheng Wang<sup>2</sup>, C. L. Wei<sup>1</sup>, D. H. Wei<sup>1</sup>, N. Wu<sup>1</sup>, X. M. Xia<sup>1</sup>, X. X. Xie<sup>1</sup>, G. F. Xu<sup>1</sup>, X. P. Xu<sup>6</sup>, Y. Xu<sup>11</sup>, M. L. Yan<sup>16</sup>, H. X. Yang<sup>1</sup>, Y. X. Yang<sup>3</sup>, M. H. Ye<sup>2</sup>, Y. X. Ye<sup>16</sup>, Z. Y. Yi<sup>1</sup>, G. W. Yu<sup>1</sup>, C. Z. Yuan<sup>1</sup>, J. M. Yuan<sup>1</sup>, Y. Yuan<sup>1</sup>, S. L. Zang<sup>1</sup>, Y. Zeng<sup>7</sup>, Yu Zeng<sup>1</sup>, B. X. Zhang<sup>1</sup>, B. Y. Zhang<sup>1</sup>, C. C. Zhang<sup>1</sup>, D. H. Zhang<sup>1</sup>, H. Q. Zhang<sup>1</sup>, H. Y. Zhang<sup>1</sup>, J. W. Zhang<sup>1</sup>, J. Y. Zhang<sup>1</sup>, S. H. Zhang<sup>1</sup>, X. M. Zhang<sup>1</sup>, X. Y. Zhang<sup>13</sup>, Yiyun Zhang<sup>14</sup>, Z. P. Zhang<sup>16</sup>, D. X. Zhao<sup>1</sup>, J. W. Zhao<sup>1</sup>, M. G. Zhao<sup>1</sup>, P. P. Zhao<sup>1</sup>, W. R. Zhao<sup>1</sup>, Z. G. Zhao<sup>1c</sup>, H. Q. Zheng<sup>12</sup>, J. P. Zheng<sup>1</sup>, Z. P. Zheng<sup>1</sup>, L. Zhou<sup>1</sup>, N. F. Zhou<sup>1c</sup>, K. J. Zhu<sup>1</sup>, Q. M. Zhu<sup>1</sup>, Y. C. Zhu<sup>1</sup>, Y. S. Zhu<sup>1</sup>, Yingchun Zhu<sup>1d</sup>, Z. A. Zhu<sup>1</sup>, B. A. Zhuang<sup>1</sup>, X. A. Zhuang<sup>1</sup>, B. S. Zou<sup>1</sup>

<sup>1</sup> Institute of High Energy Physics, Beijing 100049, People's Republic of China

<sup>2</sup> China Center for Advanced Science and Technology (CCAST), Beijing 100080, People's Republic of China

<sup>3</sup> Guangxi Normal University, Guilin 541004, People's Republic of China

<sup>4</sup> Guangxi University, Nanning 530004, People's Republic of China

<sup>5</sup> Henan Normal University, Xinxiang 453002, People's Republic of China

<sup>6</sup> Huazhong Normal University, Wuhan 430079, People's Republic of China

<sup>7</sup> Hunan University, Changsha 410082, People's Republic of China

<sup>8</sup> Jinan University, Jinan 250022, People's Republic of China

<sup>9</sup> Liaoning University, Shenyang 110036, People's Republic of China

<sup>10</sup> Nanjing Normal University, Nanjing 210097, People's Republic of China

<sup>11</sup> Nankai University, Tianjin 300071, People's Republic of China

<sup>12</sup> Peking University, Beijing 100871, People's Republic of China

<sup>13</sup> Shandong University, Jinan 250100, People's Republic of China

<sup>14</sup> Sichuan University, Chengdu 610064, People's Republic of China

<sup>15</sup> Tsinghua University, Beijing 100084, People's Republic of China

<sup>16</sup> University of Science and Technology of China, Hefei 230026, People's Republic of China

<sup>17</sup> Wuhan University, Wuhan 430072, People's Republic of China

<sup>18</sup> Zhejiang University, Hangzhou 310028, People's Republic of China

<sup>a</sup> Current address: Purdue University, West Lafayette, IN 47907, USA

<sup>b</sup> Current address: Laboratoire de l'Accélérateur Linéaire, Orsay, F-91898, France

<sup>c</sup> Current address: University of Michigan, Ann Arbor, MI 48109, USA

<sup>d</sup> Current address: DESY, D-22607, Hamburg, Germany

Received: date / Revised version: date

**Abstract.** Using the data of about  $33 \text{ pb}^{-1}$  collected at and around  $3.773 \text{ GeV}$  with the BES-II detector at the BEPC collider, we have studied the exclusive semileptonic decays  $D^+ \rightarrow K^-\pi^+e^+\nu_e$ ,  $D^0 \rightarrow \bar{K}^0\pi^-e^+\nu_e$ ,  $D^+ \rightarrow \bar{K}^{*0}e^+\nu_e$  and  $D^0 \rightarrow K^{*-}e^+\nu_e$ . The absolute branching fractions for the decays are measured to be  $BF(D^+ \rightarrow K^-\pi^+e^+\nu_e) = (3.50 \pm 0.75 \pm 0.27)\%$ ,  $BF(D^0 \rightarrow \bar{K}^0\pi^-e^+\nu_e) = (2.61 \pm 1.04 \pm 0.28)\%$ ,

## 1 Introduction

Semileptonic decays offer access to weak interaction matrix elements since the effects of weak and strong interactions can be separated reasonably well. Measurements of branching fractions for exclusive decays of  $D$  mesons play an important role to develop and to test models of their decay mechanisms.

Earlier theoretical predictions [1][2] implied that the ratio of the vector to pseudoscalar  $D$  meson semileptonic decay rates  $R = \Gamma(D \rightarrow \bar{K}^* e^+ \nu_e) / \Gamma(D \rightarrow \bar{K} e^+ \nu_e)$  lies in the range from 0.9 to 1.2 [3]. E691 Collaboration reported a measurement with a lower ratio  $\Gamma(D^+ \rightarrow \bar{K}^{*0} e^+ \nu_e) / \Gamma(D^0 \rightarrow K^- e^+ \nu_e) = 0.45 \pm 0.11$  [4], while MARK-III Collaboration obtained  $\Gamma(D \rightarrow \bar{K} \pi e^+ \nu_e) / \Gamma(D \rightarrow \bar{K} e^+ \nu_e) = 1.0_{-0.2}^{+0.3}$  [5] which is consistent with the early theoretical predictions. Since then, some controversies evolved concerning the  $R$  ratio from both theoretical predictions and experimental measurements. Contrary to the earlier expectations, recent theoretical predictions and experimental measurements tend to support a smaller value [6][7]. A compilation of predictions and experimental values can be found in [6]. The  $R$  ratio is governed by form factors of the hadronic currents. So a measurement of  $R$  is essential to test form factor calculations.

In this paper, we report direct measurements of the branching fractions for the decays  $D^+ \rightarrow K^- \pi^+ e^+ \nu_e$  (throughout this paper, charge conjugation is implied),  $D^0 \rightarrow \bar{K}^0 \pi^- e^+ \nu_e$ ,  $D^+ \rightarrow \bar{K}^{*0} e^+ \nu_e$  and  $D^0 \rightarrow K^{*-} e^+ \nu_e$  by analyzing the data sample of about  $33 \text{ pb}^{-1}$  [8][9] collected at and around the center-of-mass energy  $3.773 \text{ GeV}$  with the BES-II detector at the BEPC collider.

## 2 BES-II detector

The BES-II is a conventional cylindrical magnetic detector that is described in detail in Ref. [10]. A 12-layer Vertex Chamber (VC) surrounding a beryllium beam pipe provides input to event trigger, as well as coordinate information. A forty-layer main drift chamber (MDC) located just outside the VC yields precise measurements of charged particle trajectories with a solid angle coverage of 85% of  $4\pi$ ; it also provides ionization energy loss ( $dE/dx$ ) measurements for particle identification. Momentum resolution of  $1.7\% \sqrt{1+p^2}$  ( $p$  in  $\text{GeV}/c$ ) and  $dE/dx$  resolution of 8.5% for Bhabha scattering electrons are obtained for the data taken at  $\sqrt{s} = 3.773 \text{ GeV}$ . An array of 48 scintillation counters surrounding the MDC measures time of flight (TOF) of charged particles with a resolution of about 180 ps for electrons. Outside the TOF counters, a 12 radiation length, lead-gas barrel shower counter (BSC), operating in limited streamer mode, measures the energies of electrons and photons over 80% of the total solid angle with an energy resolution of  $\sigma_E/E = 0.22/\sqrt{E}$  ( $E$  in  $\text{GeV}$ ) and spatial resolutions of  $\sigma_\phi = 7.9 \text{ mrad}$  and  $\sigma_Z = 2.3 \text{ cm}$  for electrons. A solenoidal magnet outside the BSC provides a 0.4 T magnetic field in the central tracking region of the detector. Three double-layer muon

counters instrument the magnet flux return and serve to identify muons with momentum greater than  $500 \text{ MeV}/c$ . They cover 68% of the total solid angle.

## 3 Data analysis

The  $\psi(3770)$  resonance is produced in electron-positron ( $e^+e^-$ ) annihilation at the center-of-mass energy of about  $3.773 \text{ GeV}$ . It is believed to decay predominately into  $D^0 \bar{D}^0$  and  $D^+ D^-$  pairs. Therefore, if a  $\bar{D}$  meson is fully reconstructed (this is called a singly tagged  $\bar{D}$  meson) [8][9], the  $D$  meson must exist in the system recoiling against the singly tagged  $\bar{D}$  meson. In the system recoiling against singly tagged  $D^-$  and  $\bar{D}^0$  mesons, we select semileptonic decays  $D^+ \rightarrow K^- \pi^+ (\bar{K}^{*0}) e^+ \nu_e$  and  $D^0 \rightarrow \bar{K}^0 \pi^- (K^{*-}) e^+ \nu_e$  respectively, and measure branching fractions for the decays directly.

### 3.1 Event selection

In order to ensure the well-measured 3-momentum vectors and the reliability of the charged-particle identification, all charged tracks are required to be well reconstructed in the MDC with good helix fits, and to satisfy a geometry cut  $|\cos\theta| < 0.85$ , where  $\theta$  is the polar angle. Each track, except for those from  $K_S^0$  decays, must originate from the interaction region, which is defined by  $V_{xy} < 2.0 \text{ cm}$  and  $|V_z| < 20.0 \text{ cm}$ , where  $V_{xy}$  and  $|V_z|$  are the closest approach of the charged track in the  $xy$ -plane and  $z$  direction.

Pions and kaons are identified using the  $dE/dx$  and TOF measurements, with which the combined confidence levels ( $CL_\pi$  or  $CL_K$ ) for a pion or kaon hypotheses are calculated. A pion candidate is required to have  $CL_\pi > 0.001$ . In order to reduce misidentification, a kaon candidate is required to satisfy  $CL_K > CL_\pi$ . Electrons are identified using the  $dE/dx$ , TOF and BSC measurements, with which the combined confidence level ( $CL_e$ ) for the electron hypotheses is calculated. An electron candidate is required to have  $CL_e > 0.001$  and satisfy the relation  $CL_e / (CL_e + CL_K + CL_\pi) > 0.8$ .

Neutral kaons are reconstructed through the decay  $K_S^0 \rightarrow \pi^+ \pi^-$ . The difference between the invariant mass of  $\pi^+ \pi^-$  combinations and the  $K_S^0$  nominal mass should be less than  $20 \text{ MeV}/c^2$ .

Neutral pions are reconstructed through the decay  $\pi^0 \rightarrow \gamma\gamma$ . A good photon candidate must satisfy the following criteria: (1) the energy deposited in the BSC is greater than  $70 \text{ MeV}$ ; (2) the electromagnetic shower starts in the first 5 readout layers; (3) the angle between the photon and the nearest charged track is greater than  $22^\circ$ ; (4) the opening angle between the direction of the cluster development and the direction of the photon emission is less than  $37^\circ$ .

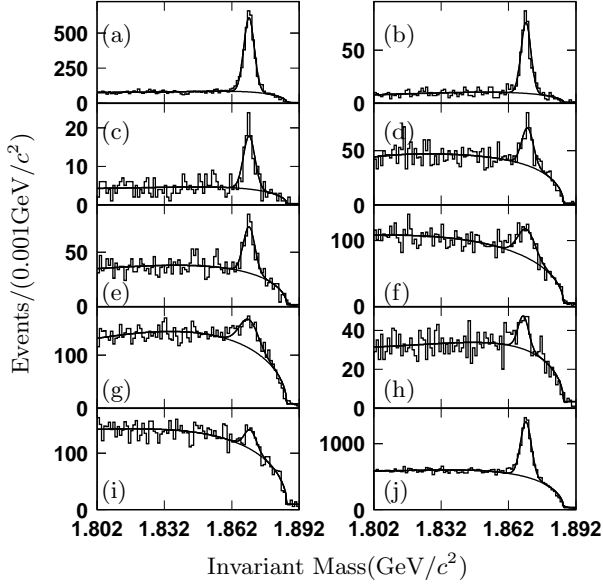


**Fig. 1.** The distributions of the fitted invariant masses of the  $nK m\pi$  ( $n = 0, 1, 2; m = 1, 2, 3, 4$ ) combinations in the singly tagged  $D^-$  modes: (a)  $K^+\pi^-\pi^-$ , (b)  $K^0\pi^-$ , (c)  $K^0K^-$ , (d)  $K^+K^-\pi^-$ , (e)  $K^0\pi^-\pi^-\pi^+$ , (f)  $K^0\pi^-\pi^0$ , (g)  $K^+\pi^-\pi^-\pi^0$ , (h)  $K^+\pi^-\pi^-\pi^-\pi^+$ , (i)  $\pi^-\pi^-\pi^+$  and (j) sum of the nine modes.

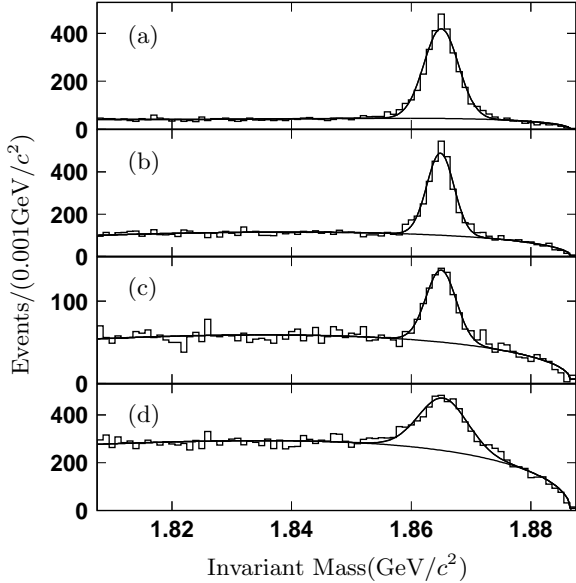


**Fig. 2.** The distributions of the fitted invariant masses of the  $K m\pi$  ( $m = 1, 2, 3$ ) combinations in the singly tagged  $\bar{D}^0$  modes: (a)  $K^+\pi^-$ , (b)  $K^+\pi^-\pi^-\pi^+$ , (c)  $K^0\pi^+\pi^-$  and (d)  $K^+\pi^-\pi^0$ .

### 3.2 Singly tagged $D^-$ and $\bar{D}^0$ samples

The singly tagged  $D^-$  and  $\bar{D}^0$  samples used in this analysis were selected in the previous work [8][9], we here give a brief description for the selection of the singly tagged  $D^-$  and  $\bar{D}^0$  samples.

The singly tagged  $D^-$  mesons are reconstructed in nine hadronic decay modes of  $K^+\pi^-\pi^-$ ,  $K^0\pi^-$ ,  $K^0K^-$ ,  $K^+K^-\pi^-$ ,  $K^0\pi^-\pi^-\pi^+$ ,  $K^0\pi^-\pi^0$ ,  $K^+\pi^-\pi^-\pi^0$ ,  $K^+\pi^-\pi^-\pi^-\pi^+$  and  $\pi^-\pi^-\pi^+$ . And the singly tagged  $\bar{D}^0$  mesons are reconstructed in four hadronic decay modes of  $K^+\pi^-$ ,  $K^+\pi^-\pi^-\pi^+$ ,  $K^0\pi^+\pi^-$  and  $K^+\pi^-\pi^0$ .

In order to improve the momentum resolution and the ratio of signal to combinatorial background in the invariant mass spectra, the center-of-mass energy constraint kinematic fit is imposed on each of the  $nK m\pi$  ( $n = 0, 1, 2; m = 1, 2, 3, 4$ ) combinations. If there is a  $K_S^0$  or  $\pi^0$  among the  $D$  daughter particles, an additional constraint kinematic fit will be imposed on the decay  $K_S^0 \rightarrow \pi^+\pi^-$  or  $\pi^0 \rightarrow \gamma\gamma$ . Combinations with a kinematic fit probability greater than 0.1% are accepted. If more than one combination satisfies the criteria in an event, only the combination with the largest fit probability is retained.

The resulting distributions of the fitted invariant masses of the  $nK m\pi$  combinations, which are calculated using the fitted momentum vectors from the kinematic fit, are shown in Fig. 1 and Fig. 2 for the singly tagged  $D^-$  and  $\bar{D}^0$  modes, respectively. A maximum likelihood fit to the mass spectrum with a Gaussian function for the  $\bar{D}$  signal and a special function [8][9] to describe the background shape yields the observed numbers of the singly tagged  $D^-$  and  $\bar{D}^0$  mesons for each mode. These give the total number of the reconstructed singly tagged  $\bar{D}$  mesons,  $5321 \pm 149 \pm 160$  for  $D^-$  [8] and  $7584 \pm 198 \pm 341$  for  $\bar{D}^0$  [9], where the first error is statistical and the second systematic obtained by varying the parameterization of the background.

### 3.3 Candidates for $D^+ \rightarrow K^-\pi^+e^+\nu_e$ and $D^0 \rightarrow \bar{K}^0\pi^-e^+\nu_e$

Candidates for the semileptonic decays  $D^+ \rightarrow K^-\pi^+e^+\nu_e$  and  $D^0 \rightarrow \bar{K}^0\pi^-e^+\nu_e$  are selected from the surviving tracks in the system recoiling against the singly tagged  $\bar{D}$  mesons. For the selected candidate events, it is required that there should be no extra charged track or isolated photon, which has not been used in the reconstruction of the singly tagged  $\bar{D}$  mesons. The isolated photon detected in the BSC should have an energy exceeding 100 MeV and should satisfy the photon selection criteria described earlier. There are possible hadronic backgrounds for each semileptonic decay due to misidentification of a charged pion as an electron, for example, the decay  $D^+ \rightarrow K^-\pi^+\pi^+$  ( $D^0 \rightarrow \bar{K}^0\pi^+\pi^-$ ) could be misidentified as  $D^+ \rightarrow K^-\pi^+e^+\nu_e$  ( $D^0 \rightarrow \bar{K}^0\pi^-e^+\nu_e$ ). However, these events can be suppressed by requiring the invariant masses of  $K^-\pi^+e^+$  ( $\bar{K}^0\pi^-e^+$ ) combinations to be less than  $1.75 \text{ GeV}/c^2$ .

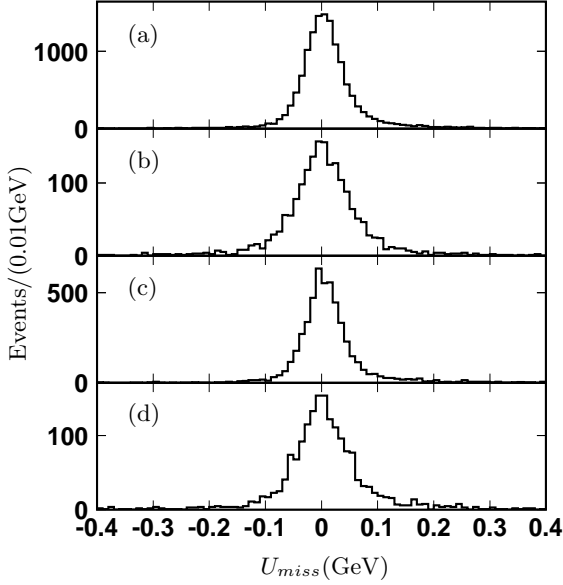


**Fig. 3.** The distributions of the  $U_{miss}$  for the Monte Carlo events of (a)  $D^+ \rightarrow K^- \pi^+ e^+ \nu_e$  versus  $D^- \rightarrow K^+ \pi^- \pi^-$ , (b)  $D^+ \rightarrow K^- \pi^+ e^+ \nu_e$  versus  $D^- \rightarrow K^+ \pi^- \pi^- \pi^0$ , (c)  $D^0 \rightarrow \bar{K}^0 \pi^- e^+ \nu_e$  versus  $\bar{D}^0 \rightarrow K^+ \pi^-$  and (d)  $D^0 \rightarrow \bar{K}^0 \pi^- e^+ \nu_e$  versus  $\bar{D}^0 \rightarrow K^+ \pi^- \pi^0$ .

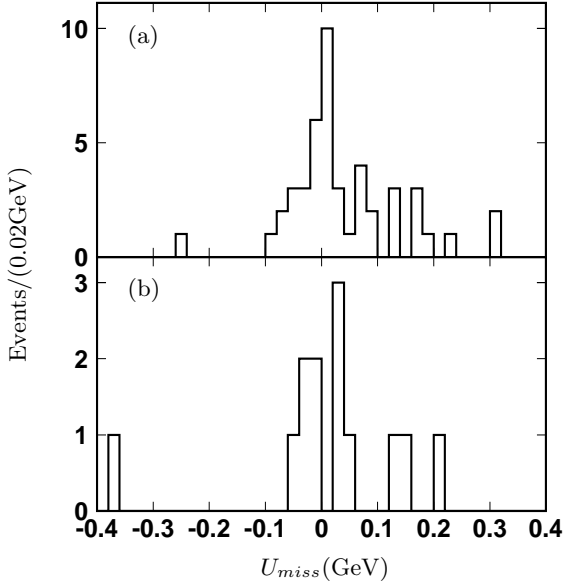


**Fig. 4.** The distributions of the  $U_{miss}$  for the selected candidates for (a)  $D^+ \rightarrow K^- \pi^+ e^+ \nu_e$  and (b)  $D^0 \rightarrow \bar{K}^0 \pi^- e^+ \nu_e$  from the data.

In the semileptonic decays, there is one massless neutrino which is undetected. To obtain information about missing neutrinos, a kinematic quantity  $U_{miss} \equiv E_{miss} - p_{miss}$  is used [8][9], where  $E_{miss}$  and  $p_{miss}$  are the total energy and momentum of all missing particles. To select the semileptonic decays, it is required that the candidates for the semileptonic decays should have their  $|U_{miss,i}| <$

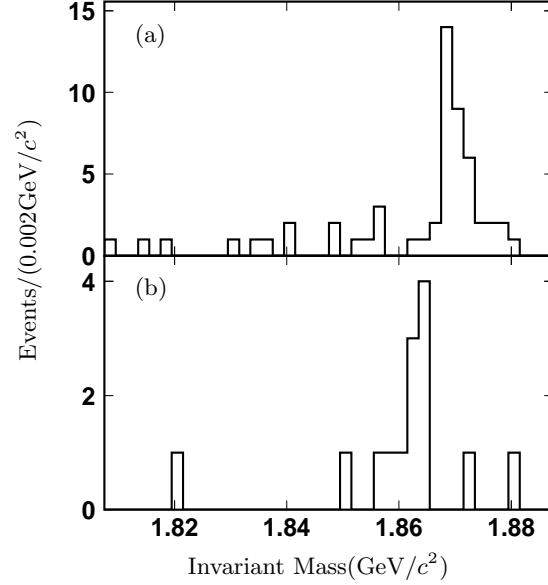


**Fig. 5.** The distributions of the fitted invariant masses of the  $nK m \pi$  combinations for the events in which the candidates for (a)  $D^+ \rightarrow K^- \pi^+ e^+ \nu_e$  and (b)  $D^0 \rightarrow \bar{K}^0 \pi^- e^+ \nu_e$  are observed in the system recoiling against the singly tagged  $\bar{D}$ .

$3\sigma_{U_{miss,i}}$ , where the  $\sigma_{U_{miss,i}}$  is the standard deviation of the  $U_{miss,i}$  distribution obtained by analyzing the Monte Carlo events of  $D^+ \rightarrow K^- \pi^+ e^+ \nu_e$  ( $D^0 \rightarrow \bar{K}^0 \pi^- e^+ \nu_e$ ) versus the  $i$ th singly tagged  $\bar{D}$  mode. Fig. 3 shows the distributions of the  $U_{miss}$ , with each peak centered at zero as expected, for the Monte Carlo events of  $D^+ \rightarrow K^- \pi^+ e^+ \nu_e$  versus  $D^- \rightarrow K^+ \pi^- \pi^-$ ,  $D^+ \rightarrow K^- \pi^+ e^+ \nu_e$  versus  $D^- \rightarrow K^+ \pi^- \pi^- \pi^0$ ,  $D^0 \rightarrow \bar{K}^0 \pi^- e^+ \nu_e$  versus  $\bar{D}^0 \rightarrow K^+ \pi^-$  and  $D^0 \rightarrow \bar{K}^0 \pi^- e^+ \nu_e$  versus  $\bar{D}^0 \rightarrow K^+ \pi^- \pi^0$ , respectively. Fig. 4(a) and Fig. 4(b) respectively show the distributions of the  $U_{miss}$  for the selected candidates for  $D^+ \rightarrow K^- \pi^+ e^+ \nu_e$  and  $D^0 \rightarrow \bar{K}^0 \pi^- e^+ \nu_e$  from the data.

Figure 5 shows the distributions of the fitted invariant masses of the  $nK m \pi$  combinations from the events in which the candidates for  $D^+ \rightarrow K^- \pi^+ e^+ \nu_e$  and  $D^0 \rightarrow \bar{K}^0 \pi^- e^+ \nu_e$  are selected in the system recoiling against the  $nK m \pi$  combinations. Fig. 5(a) indicates that an obvious signal of  $D^+ \rightarrow K^- \pi^+ e^+ \nu_e$  via the  $D^-$  tags is observed. There are 37 events in the  $\pm 3\sigma_{M_{D_i}}$  mass window of the fitted  $D$  meson mass  $M_{D_i}$ , and 18 events in the outside of the signal regions, where  $\sigma_{M_{D_i}}$  is the standard deviation of the  $nK m \pi$  distribution for the  $i$ th mode. By assuming that the distribution of background is flat,  $5.6 \pm 1.4$  background events in the signal regions are estimated. After subtracting the number of background events,  $31.4 \pm 6.2$  candidates for  $D^+ \rightarrow K^- \pi^+ e^+ \nu_e$  are retained. A similar analysis of the events in Fig. 5(b) yields  $9.9 \pm 3.4$  candidates for  $D^0 \rightarrow \bar{K}^0 \pi^- e^+ \nu_e$ . There may also be the  $\pi^+ \pi^-$  combinatorial background. By selecting the events in which the invariant masses of the  $\pi^+ \pi^-$  combinations on the recoil side of the tags are outside of the  $K_S^0$  mass

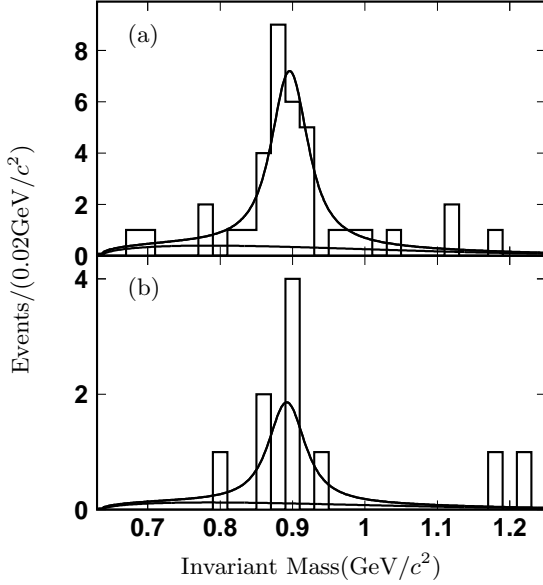


**Fig. 6.** The distributions of the invariant masses of (a)  $K^- \pi^+$  combinations from the selected candidates for  $D^+ \rightarrow \bar{K}^{*0} e^+ \nu_e$  and (b)  $\bar{K}^0 \pi^-$  combinations from the selected candidates for  $D^0 \rightarrow K^{*-} e^+ \nu_e$ .

window, we estimate that there are  $0.6 \pm 0.2$  background events in the candidate events. After subtracting the number of background events,  $9.3 \pm 3.4$  candidate events are retained.

### 3.4 Candidates for $D^+ \rightarrow \bar{K}^{*0} e^+ \nu_e$ and $D^0 \rightarrow K^{*-} e^+ \nu_e$

To select the candidates for  $D^+ \rightarrow \bar{K}^{*0} e^+ \nu_e$  and  $D^0 \rightarrow K^{*-} e^+ \nu_e$ , we calculate the invariant masses of  $K^- \pi^+$  ( $\bar{K}^0 \pi^-$ ) combinations from the selected candidates for  $D^+ \rightarrow K^- \pi^+ e^+ \nu_e$  ( $D^0 \rightarrow \bar{K}^0 \pi^- e^+ \nu_e$ ). Fig. 6(a) and Fig. 6(b) show the distributions of the invariant masses of  $K^- \pi^+$  and  $\bar{K}^0 \pi^-$  combinations for the events in which the invariant masses of the  $nK\pi$  combinations are within the  $\pm 3\sigma_{M_{D_i}}$  mass window of the fitted  $D$  meson mass  $M_{D_i}$ . A clear  $\bar{K}^{*0}$  signal is observed in Fig. 6(a). Fitting the  $K^- \pi^+$  invariant mass spectrum with a Gaussian function for the  $\bar{K}^{*0}$  signal and a S-wave  $K\pi$  phase space background shape, we obtain  $29.1 \pm 6.6$  candidates for  $D^+ \rightarrow \bar{K}^{*0} e^+ \nu_e$ . In the fit, the mass and width of  $\bar{K}^{*0}$  are respectively fixed to  $0.8961 \text{ GeV}/c^2$  and  $50.7 \text{ MeV}/c^2$  quoted from PDG [11], the mass resolution is fixed to  $10 \text{ MeV}/c^2$  determined by Monte Carlo simulation. Using the same background shape, a similar fit to the  $\bar{K}^0 \pi^-$  invariant mass spectrum in Fig. 6(b) yields  $7.4 \pm 3.3$  candidates for  $D^0 \rightarrow K^{*-} e^+ \nu_e$ . After subtracting the number of  $\pi^+ \pi^-$  combinatorial background of  $0.1 \pm 0.1$  events,  $7.3 \pm 3.3$  candidate events are retained.

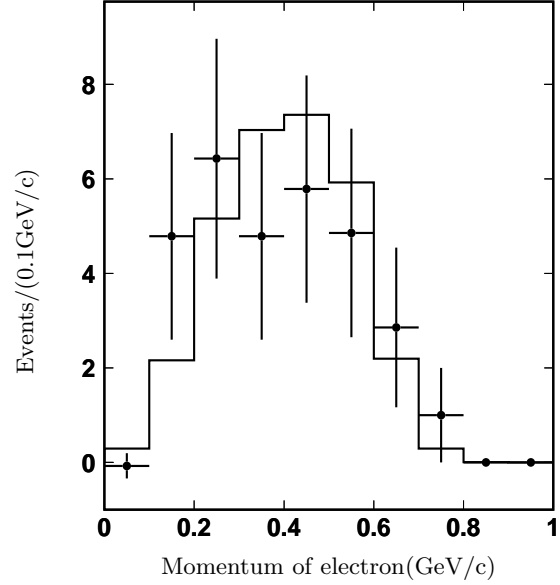


**Fig. 7.** The distribution of the momentum of the electrons from the selected candidates for  $D^+ \rightarrow \bar{K}^{*0} e^+ \nu_e$ , where the points with error bars are from the data and histogram is from the Monte Carlo events of  $D^+ \rightarrow \bar{K}^{*0} e^+ \nu_e$ .

However, there are still some  $K^*$  contaminations from other modes of  $D$  meson decays or from continuum background due to the combinatorial background in the singly tagged  $\bar{D}$  signal regions. These  $K^*$  contaminations must be subtracted from the fitted number of the selected candidates for  $D^+ \rightarrow \bar{K}^{*0} e^+ \nu_e$  and  $D^0 \rightarrow K^{*-} e^+ \nu_e$ . They are estimated by using the  $\bar{D}$  sideband events. The numbers of the events satisfying the selection criteria in the  $\bar{D}$  sideband are then normalized to obtain the numbers of the background events in the  $\bar{D}$  signal regions. Totally  $0.8 \pm 0.8$  and  $0.7 \pm 0.5$  background events for  $D^+ \rightarrow \bar{K}^{*0} e^+ \nu_e$  and  $D^0 \rightarrow K^{*-} e^+ \nu_e$  are obtained respectively. After subtracting the numbers of the background events,  $28.3 \pm 6.6$  and  $6.6 \pm 3.3$  candidate events for  $D^+ \rightarrow \bar{K}^{*0} e^+ \nu_e$  and  $D^0 \rightarrow K^{*-} e^+ \nu_e$  are respectively retained.

The distribution of the momentum of the electrons from the selected candidates for  $D^+ \rightarrow \bar{K}^{*0} e^+ \nu_e$  is shown in Fig. 7, where the points with error bars are from the data and the histogram is from the Monte Carlo events of  $D^+ \rightarrow \bar{K}^{*0} e^+ \nu_e$ . The contaminations from hadronic and some other semileptonic decays have been subtracted from the observed events based on study of the Monte Carlo events of  $e^+ e^- \rightarrow D\bar{D}$ .

### 3.5 Other backgrounds

The events from other hadronic or semileptonic decays may also satisfy the selection criteria for the semileptonic decays and are misidentified as the semileptonic decay events. The numbers of the misidentified events have to be subtracted from the candidates for the semileptonic decays. The numbers of the background events are estimated

by analyzing the Monte Carlo sample which is about 14 times larger than the data. The Monte Carlo events are generated as  $e^+e^- \rightarrow D\bar{D}$ , where the  $D$  and  $\bar{D}$  mesons are set to decay into all possible final states with the branching fractions quoted from PDG [11] excluding the decay modes under study. The particle trajectories are simulated with the GEANT3 based Monte Carlo simulation package for the BES-II detector [12]. The number of the events satisfying the selection criteria is then normalized to the data. Monte Carlo study shows that the dominant background for  $D^+ \rightarrow K^-\pi^+(\bar{K}^{*0})e^+\nu_e$  is from  $D^+ \rightarrow \bar{K}^{*0}\mu^+\nu_\mu$ , and the background for  $D^0 \rightarrow \bar{K}^0\pi^-(K^{*-})e^+\nu_e$  is from  $D^0 \rightarrow K^{*-}\pi^+$ . Totally  $2.5 \pm 0.5$ ,  $0.8 \pm 0.3$ ,  $0.7 \pm 0.3$  and  $0.2 \pm 0.3$  background events for  $D^+ \rightarrow K^-\pi^+e^+\nu_e$ ,  $D^0 \rightarrow \bar{K}^0\pi^-e^+\nu_e$ ,  $D^+ \rightarrow \bar{K}^{*0}e^+\nu_e$  and  $D^0 \rightarrow K^{*-}e^+\nu_e$  are obtained, respectively. After subtracting the numbers of the background events,  $28.9 \pm 6.2$ ,  $8.5 \pm 3.4$ ,  $27.6 \pm 6.6$  and  $6.4 \pm 3.3$  signal events for the semileptonic decays  $D^+ \rightarrow K^-\pi^+e^+\nu_e$ ,  $D^0 \rightarrow \bar{K}^0\pi^-e^+\nu_e$ ,  $D^+ \rightarrow \bar{K}^{*0}e^+\nu_e$  and  $D^0 \rightarrow K^{*-}e^+\nu_e$  are obtained.

## 4 Results

### 4.1 Monte Carlo efficiency

The detection efficiencies for the semileptonic decays  $D^+ \rightarrow K^-\pi^+e^+\nu_e$ ,  $D^0 \rightarrow \bar{K}^0\pi^-e^+\nu_e$ ,  $D^+ \rightarrow \bar{K}^{*0}e^+\nu_e$  and  $D^0 \rightarrow K^{*-}e^+\nu_e$  are estimated to be  $\epsilon_{D^+ \rightarrow K^-\pi^+e^+\nu_e} = (15.51 \pm 0.12)\%$ ,  $\epsilon_{D^0 \rightarrow \bar{K}^0\pi^-e^+\nu_e} = (4.30 \pm 0.05)\%$ ,  $\epsilon_{D^+ \rightarrow \bar{K}^{*0}e^+\nu_e} = (10.26 \pm 0.08)\%$  and  $\epsilon_{D^0 \rightarrow K^{*-}e^+\nu_e} = (2.94 \pm 0.04)\%$  by Monte Carlo simulation, which include the branching fractions for the intermediate sub-resonance decays.

### 4.2 Branching fractions

The branching fraction for the semileptonic decay  $D \rightarrow j$  (where  $j = K^-\pi^+e^+\nu_e$ ,  $\bar{K}^0\pi^-e^+\nu_e$ ,  $\bar{K}^{*0}e^+\nu_e$  and  $K^{*-}e^+\nu_e$ ) can be determined by

$$BF(D \rightarrow j) = \frac{N_{D \rightarrow j}}{N_{\bar{D}tag} \times \epsilon_{D \rightarrow j}}, \quad (1)$$

where  $N_{D \rightarrow j}$  is the number of the signal events for the  $j$ th mode;  $N_{\bar{D}tag}$  is the total number of the singly tagged  $D^-$  or  $\bar{D}^0$  mesons;  $\epsilon_{D \rightarrow j}$  is the detection efficiency for the  $j$ th mode. Inserting these numbers in Eq. (1), we obtain the branching fractions for the semileptonic decays to be

$$BF(D^+ \rightarrow K^-\pi^+e^+\nu_e) = (3.50 \pm 0.75 \pm 0.27)\%,$$

$$BF(D^0 \rightarrow \bar{K}^0\pi^-e^+\nu_e) = (2.61 \pm 1.04 \pm 0.28)\%,$$

$$BF(D^+ \rightarrow \bar{K}^{*0}e^+\nu_e) = (5.06 \pm 1.21 \pm 0.40)\%$$

and

$$BF(D^0 \rightarrow K^{*-}e^+\nu_e) = (2.87 \pm 1.48 \pm 0.39)\%,$$

where the first error is statistical and the second systematic. The systematic error arises mainly from the uncertainties in tracking efficiency ( $\sim 2.0\%$  per track), in particle identification ( $\sim 0.5\%$  per track for charged pion or kaon,  $\sim 1.0\%$  per track for electron), in photon selection ( $\sim 2.0\%$ ), in  $K_S^0$  selection ( $\sim 1.1\%$ ), in  $U_{miss}$  selection ( $\sim 0.6\%$ ), in background subtraction [ $\sim (2.5\% \sim 9.3\%)$ ], in Monte Carlo statistics [ $\sim (0.8\% \sim 1.4\%)$ ], in the number of the singly tagged  $\bar{D}$  mesons ( $\sim 3.0\%$  for  $D^-$  and  $\sim 4.5\%$  for  $\bar{D}^0$ ) and in the fit to the mass spectrum of  $K^-\pi^+$  or  $\bar{K}^0\pi^-$  combination ( $\sim 1.7\%$  for  $D^+ \rightarrow \bar{K}^{*0}e^+\nu_e$  and  $\sim 2.5\%$  for  $D^0 \rightarrow K^{*-}e^+\nu_e$ ). These uncertainties are added in quadrature to obtain the total systematic error, yielding  $\sim 7.6\%$ ,  $\sim 10.8\%$ ,  $\sim 8.0\%$  and  $\sim 13.7\%$  for the semileptonic decays  $D^+ \rightarrow K^-\pi^+e^+\nu_e$ ,  $D^0 \rightarrow \bar{K}^0\pi^-e^+\nu_e$ ,  $D^+ \rightarrow \bar{K}^{*0}e^+\nu_e$  and  $D^0 \rightarrow K^{*-}e^+\nu_e$ , respectively.

### 4.3 The ratio of $\frac{\Gamma(D^+ \rightarrow \bar{K}^{*0}e^+\nu_e)}{\Gamma(D^+ \rightarrow \bar{K}^0e^+\nu_e)}$

With the measured branching fraction for  $D^+ \rightarrow \bar{K}^{*0}e^+\nu_e$  and the previously measured branching fraction  $BF(D^+ \rightarrow \bar{K}^0e^+\nu_e) = (8.95 \pm 1.59 \pm 0.67)\%$  by BES Collaboration [8], we obtain the ratio of the vector to pseudoscalar  $D$  meson semileptonic decay rates to be

$$\frac{\Gamma(D^+ \rightarrow \bar{K}^{*0}e^+\nu_e)}{\Gamma(D^+ \rightarrow \bar{K}^0e^+\nu_e)} = 0.57 \pm 0.17 \pm 0.02,$$

where the first error is statistical and the second systematic which arises mainly from the uncanceled systematic uncertainties including  $K_S^0$  selection ( $\sim 1.1\%$ ), background subtraction ( $\sim 3.5\%$ ), Monte Carlo statistics ( $\sim 1.1\%$ ) and the fit to the mass spectrum of  $K^-\pi^+$  combinations ( $\sim 1.7\%$ ).

## 5 Summary

Using the data of about  $33 \text{ pb}^{-1}$  collected around  $3.773 \text{ GeV}$  with the BES-II detector at the BEPC collider, the absolute branching fractions for the decays  $D^+ \rightarrow K^-\pi^+e^+\nu_e$ ,  $D^0 \rightarrow \bar{K}^0\pi^-e^+\nu_e$ ,  $D^+ \rightarrow \bar{K}^{*0}e^+\nu_e$  and  $D^0 \rightarrow K^{*-}e^+\nu_e$  are measured to be  $BF(D^+ \rightarrow K^-\pi^+e^+\nu_e) = (3.50 \pm 0.75 \pm 0.27)\%$ ,  $BF(D^0 \rightarrow \bar{K}^0\pi^-e^+\nu_e) = (2.61 \pm 1.04 \pm 0.28)\%$ ,  $BF(D^+ \rightarrow \bar{K}^{*0}e^+\nu_e) = (5.06 \pm 1.21 \pm 0.40)\%$  and  $BF(D^0 \rightarrow K^{*-}e^+\nu_e) = (2.87 \pm 1.48 \pm 0.39)\%$ . With the measured branching fraction for  $D^+ \rightarrow \bar{K}^{*0}e^+\nu_e$  and the previously measured branching fraction for  $D^+ \rightarrow \bar{K}^0e^+\nu_e$ , the ratio of the vector to pseudoscalar  $D$  meson semileptonic decay rates  $\Gamma(D^+ \rightarrow \bar{K}^{*0}e^+\nu_e)/\Gamma(D^+ \rightarrow \bar{K}^0e^+\nu_e)$  is determined to be  $0.57 \pm 0.17 \pm 0.02$ , which is in good agreement with theoretical predictions and other measurements [6][7] within error.

## 6 Acknowledgment

The BES collaboration thanks the staff of BEPC and computing center for their hard efforts. This work is supported in part by the National Natural Science Foundation of China under contracts Nos. 10491300, 10225524, 10225525, 10425523, the Chinese Academy of Sciences under contract No. KJ 95T-03, the 100 Talents Program of CAS under Contract Nos. U-11, U-24, U-25, and the Knowledge Innovation Project of CAS under Contract Nos. U-602, U-34 (IHEP), the National Natural Science Foundation of China under Contract No. 10225522 (Tsinghua University).

## References

1. M. Wirbel, B. Stech and M. Baucer, *Z. Phys.* **C** 29 (1985) 637.
2. V. Lubicz et. al, *Phys. Lett.* **B** 274 (1992) 415.
3. J.D. Richman and P.R. Burchat, *Rev. Mod. Phys.* 67 (1995) 893.
4. The Tagged Photon Spectrometer Collaboration, J.C. Anjos et al., *Phys. Rev. Lett.* 62 (1989) 722.
5. Mark III Collaboration, Z. Bai et al., *Phys. Rev. Lett.* 66 (1991) 1011.
6. FOCUS Collaboration, J.M. Link et al., *Phys. Lett.* **B** 598 (2004) 33.
7. CLEO Collaboration, G.S. Huang et al., *Phys. Rev. Lett.* 95 (2005) 181801.
8. BES Collaboration, M. Ablikim, et al., *Phys. Lett.* **B** 608 (2005) 24.
9. BES Collaboration, M. Ablikim, et al., *Phys. Lett.* **B** 597 (2004) 39.
10. BES Collaboration, J.Z. Bai et al., *Nucl. Instrum. Methods* **A** 458 (2001) 627.
11. S. Eidelman et al. (Particle Data Group), *Phys. Lett.* **B** 592 (2004) 1.
12. BES Collaboration, M. Ablikim, et al., *Nucl. Instrum. Methods* **A** 552 (2005) 344.